

# Helicopters Aircraft Engines Self-Organizing Neural Network Automatic Control System

Serhii Vladov<sup>a</sup>, Yurii Shmelov<sup>a</sup> and Ruslan Yakovliev<sup>a</sup>

<sup>a</sup> *Kremenchuk Flight College of Kharkiv National University of Internal Affairs, vul. Peremohy, 17/6, Kremenchuk, Poltavaska Oblast, Ukraine, 39605*

## Abstract

The purpose of this work is to dedicate to the improvement of the automatic control system for helicopters aircraft engines by dividing the control object into actuating mechanism and gas turbine engine. This allows you to take into account the dynamics of the executive part of the system and the engine, it becomes possible to use the mismatch between parts of the structural diagram of the automatic control system, thereby increasing the reliability and stability of the system in various modes. As a hardware-software implementation of the automatic control system for helicopters aircraft engines, it is proposed to use a self-tuning neural network control system for multiply connected dynamic objects, the adaptation of which as a modified neural network controller of helicopters aircraft engines by introducing an integrator into the system structure made it possible to bring the graph of the real transient process in the engine closer to the ideal one, thereby increasing the reliability and stability of the system in various modes.

## Keywords

Helicopter aircraft engine, automatic control system, neural network, transfer function, transient processes.

## 1. Introduction

The process of ensuring the stability of the operation parameters of helicopters aircraft turboshaft engines (TE) by maintaining the required (stable) compressor rotor speed and the dosage of fuel supply to the combustion chamber has always been a difficult task. Of particular difficulty are the launch modes and transient modes of engine operation, taking into account external factors (the impact of atmospheric conditions and aircraft flight modes). In view of this, automatic control systems (ACS) are used to adjust the engine [1, 2]. The values of engine thermogasdynamic parameters required for helicopter flight and the reliable and stable operation of the power plant over the entire range of operating conditions are ensured with appropriate engine adjustment carried out by the ACS. It establishes and maintains some relationships between engine parameters. This regulation is formed taking into account the requirements for specific fuel consumption and other thermogasdynamic parameters, strength limitations, the required accuracy of maintaining parameters, and other factors [3, 4].

At present, the ACS of TE that implement the specified control laws are subject to rather stringent requirements both for permissible deviations of parameters in steady-state operating modes and for dynamic errors during transients [5]. The ACS for helicopters TE is no exception. As a rule, the following requirements are imposed of TE ACS: high accuracy of maintaining the specified parameters; minimal complexity of technical execution; the possibility of switching from one mode to

---

CMIS-2022: The Fifth International Workshop on Computer Modeling and Intelligent Systems, Zaporizhzhia, Ukraine, May 12, 2022  
EMAIL: ser26101968@gmail.com (S. Vladov); nviddil.klk@gmail.com (Yu. Shmelov); ateu.nv.klk@gmail.com (R. Yakovliev)  
ORCID: 0000-0001-8009-5254 (S. Vladov); 0000-0002-3942-2003 (Yu. Shmelov); 0000-0002-3788-2583 (R. Yakovliev)



© 2022 Copyright for this paper by its authors.  
Use permitted under Creative Commons License Attribution 4.0 International (CC BY 4.0).  
CEUR Workshop Proceedings (CEUR-WS.org)

another (when performing a maneuver) without reducing the quality of control. To fulfill all the above requirements, it is necessary to create a new approach to the choice of the ACS structure, the synthesis of control methods and their technical implementation. This statement is based on the analysis of the results of full-scale tests and previous theoretical studies.

## 2. Literature review

Modern methods and experience in development automatic control systems for gas turbine engines originate in the works of scientists, for example, A. Shevyakov, S. Sirotin, O. Gurevich, F. Golberg, O. Selivanov, G. Dobryansky, V. Dedesh, V. Rutkovsky, S. Zemlyakov, B. Petrov, B. Cherkasov, V. Avgustinovich, Yu. Gusev, F. Shaimardanov, B. Ilyasov, V. Vasiliev, G. Kulikov, Yu. Kabalnov, V. Krymsky, V. Efanov and others. Problems of scientists from foreign universities, research organizations and firms involved in the creation of dynamic objects, engines and airborne equipment.

In many practical cases, it becomes necessary to automate processes occurring in complex dynamic systems, which include several subsystems that are interconnected and interact with each other [6]. The characteristic properties of such systems are non-linearity, multidimensionality, multi-connectivity and multifunctionality, i.e., during normal operation, both the layout of the system and the dynamic properties of the separate subsystems themselves change [7]. Examples of such modern systems are multi-connected automatic control systems (MCAS) for complex dynamic objects, such as aircraft gas turbine engine, power complexes, synchronous generators, and so on. According to the American company Honeywell, which analyzed the operation of more than 100000 control loops in 350 production processes, about 49 % of the control loops are configured incorrectly or erroneously [8]. The main difficulty in this case lies in ensuring the stability and the desired quality of functioning of both the MCAS as a whole and its separate subsystems in various operating modes [9]. Therefore, achieving the desired quality of functioning of a multiply connected system is an urgent practical and theoretical task. In the article, to solve this problem, it is proposed to use logical controllers in separate channels.

In modern MCAS, to improve the dynamic properties, nonlinear elements and connections are often used, implemented in the form of nonlinear controllers [10]. The use of nonlinear algorithms significantly expands the possibilities of purposefully changing the quality of control processes, and also improves the dynamic and static properties of the system [11].

Among this class of regulators, regulators with logical switching of transmission coefficients either in a direct circuit or in a feedback circuit are widely used [12]. Switching in such systems occurs at certain ratios of the coordinates of the system, which are determined by the logical control law. There are many different logical control laws [13–15], which have in common that switching occurs depending on the value of the error coordinate  $\varepsilon(t)$  and its derivative  $\varepsilon'(t)$ . However, these logic control laws are developed for systems with one input and output, and do not take into account the mutual influence of separate channels, which is typical for MCAS. And also, for them it is necessary to calculate the values of the coefficients each time when the parameters of the control object change to ensure high quality control. Under these conditions, the use of the apparatus of neural networks is appropriate.

## 3. Synthesis of a multidimensional neural network controller for helicopters aircraft turboshaft engines

It is assumed that the dynamic properties of helicopters aircraft TE as multidimensional control objects are described by the following differential equations "input-output":

$$\varphi = \left( \mathbf{Y}^{(n)}, \mathbf{Y}^{(n-1)}, \dots, \mathbf{Y}; \mathbf{U}^{(n)}, \mathbf{U}^{(n-1)}, \dots, \mathbf{U} \right); \quad (1)$$

where  $\mathbf{U} = (u_1(t), u_2(t), \dots, u_N(t))^T$ ,  $\mathbf{Y} = (y_1(t), y_2(t), \dots, y_N(t))^T$  – respectively, vectors of inputs (control actions) and outputs (controlled variables);  $m$  and  $n$  – maximum orders of derivatives  $u_k^{(i)}$ ,

$y_e^{(j)}$  for input and output variables  $u_k(t)$  and  $y_e(t)$ , ( $m \leq n$ );  $N$  – number of engine control channels, that is, the dimension of the ACS;  $\varphi(\cdot)$  – nonlinear vector function.

It is also considered that for helicopters aircraft TE, the condition of observation and control is made [16]. In [17–19], a block diagram of a multidimensional ACS for helicopters aircraft TE (using the TV3-117 aircraft engine as an example) is proposed with the inclusion of  $N$  integrators (I) in the system – one in each of the  $N$  channels of the control system (fig. 1), implemented in in the form of a multi-mode neural network controller using a dynamic recurrent neural network based on a perceptron (fig. 2), which provides control of the object (1), subject to the following requirements for the synthesized ACS:

- astaticism (zero static error);
- physical implementation of the neural network controller;
- stability and given quality of control processes on a fixed set of modes  $M = \{M_1, \dots, M_R\}$  of engine operation;
- minimum complexity of the multidimensional neural network controller.

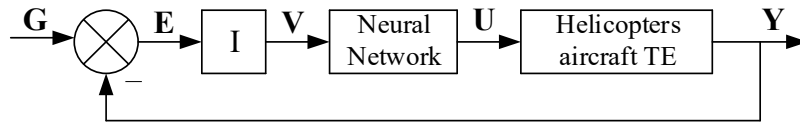


**Figure 1:** Structural diagram of the multidimensional ACS of helicopters aircraft TE

The requirement of astaticism of a multidimensional ACS is reduced to the inclusion of  $N$  integrators (I) in the system – one in each of the  $N$  channels of the control system. Then for the circuit in fig. 1 can be accepted:

$$V_i(z) = \frac{T_0}{1-z^{-1}} E_i(z); \quad (2)$$

where  $i = 1, 2, \dots, N$ ;  $z^{-1}$  – time shift operator, one cycle delay  $T_0$ ;  $\frac{T_0}{1-z^{-1}}$  – integrator discrete transfer function.

The requirement of the physical capability of the neural network controller to be implemented is based on the assumption that a dynamic recurrent neural network based on a perceptron is taken as a neural network (fig. 2).

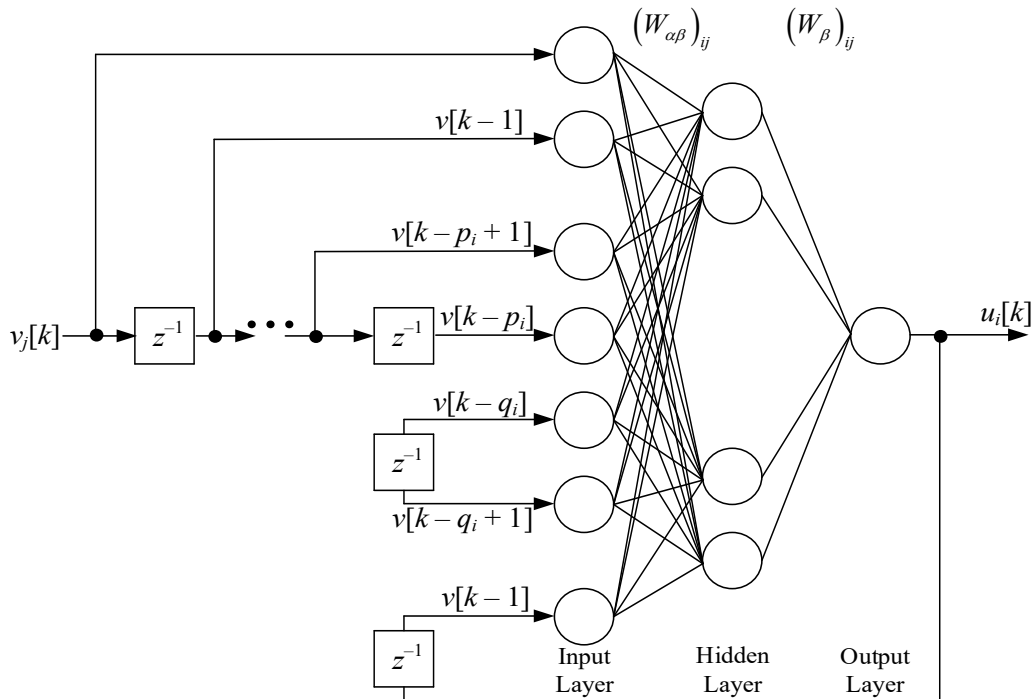


**Figure 2:** Multimode neural network controller based on perceptron

The neural network controller has  $N$  inputs and  $N$  outputs, including  $N + \sum_{i=1}^N (p_i + q_i)$  neurons in the input layer,  $\sigma$  neurons in the common hidden layer, and  $N$  neurons in the output layer, the connections between which are carried out using adjustable (training) weights  $W_{\alpha\beta}$ ,  $W_{\beta}$  ( $\alpha = 1, 2, \dots, N + \sum_{i=1}^N (p_i + q_i)$ ;  $\beta = 1, 2, \dots, N_{\sigma}$ ). It is obvious that the number of neurons in the hidden layer  $\sigma$  must satisfy the constraints  $\sigma > N$  (otherwise, it is impossible to provide independent formation of control actions  $u_1, u_2, \dots, u_N$  when changing the neural network inputs  $v_1, v_2, \dots, v_N$ ) [17–19]. The total number of unknown parameters of the neural network controller, that is, the number of adjustable neural network weights, is:

$$K_p = \sigma \left( 2N + \sum_{i=1}^N (p_i + q_i) \right). \quad (3)$$

To ensure stability on a given set of  $M_1, \dots, M_R$  modes of operation of helicopter aircraft TE ACS, it is necessary to fulfill the following relationship between the values of  $p_i, q_i, \sigma, n, R$  and  $N$ :

$$\sigma \left( 2N + \sum_{i=1}^N p_i \right) + (\sigma - R) \sum_{i=1}^N q_i \geq R(N + n); \quad (4)$$

from which it is possible to determine the unknown integer values  $p_i, q_i$  and  $\sigma$ , which determine the structure of the neural network controller.

To fulfill the requirement of the minimum complexity criterion, it is assumed that the complexity of the neural network controller is determined by the number of adjustable neural network parameters ( $K_p$ ), the desired solution to the structural synthesis problem based on the minimum complexity criterion should be considered a neural network controller described by a set of numbers  $\langle p_1, \dots, p_N; q_1, \dots, q_N; \sigma \rangle$  minimizing the value of the objective function (3) when executing the constraint (4).

For helicopters aircraft TE, the vector of inputs (control actions) has the form:

$$\mathbf{U} = (G_T)^T; \quad (5)$$

where  $G_T$  – fuel consumption, and the state vector and the vector of outputs (controlled variables) of the engine are written, respectively, as  $\mathbf{X} = (x_1, x_2)^T$  and  $\mathbf{Y} = (n_{TC}, T_G^*)$ , where  $n_{TC}$  – gas generator r.p.m.;  $T_G^*$  – gas temperature in front of the compressor turbine.

The block diagram of the ACS is shown in fig. 3, where  $D_n$  and  $D_T$  – sensors gas generator r.p.m. and gas temperature in front of the compressor turbine;  $Act_{G_T}$  – actuator that provides the formation of actions along the coordinate  $\overline{G_T}$ ;  $\mathbf{G} = \begin{pmatrix} \overline{n_{TC}}^0 \\ \overline{T_G}^0 \end{pmatrix}^T$  – vector of settings (given influences);  $\overline{n_{TC}}^0$  and  $\overline{T_G}^0$  – required (tasks) values gas generator r.p.m.;  $T_G^*$  – gas temperature in front of the compressor turbine.

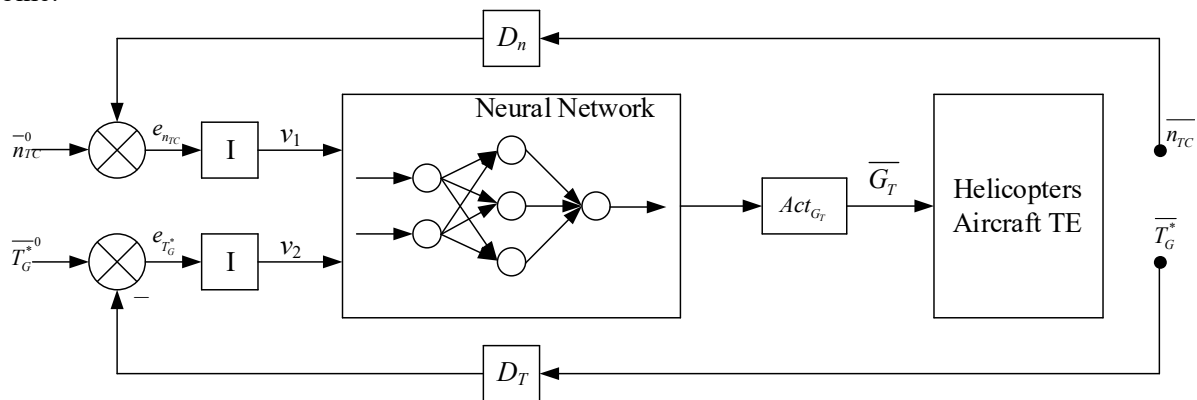


**Figure 3:** Structural diagram of synthesized ACS for helicopters aircraft TE

#### 4. Modification of automatic control system for helicopters turboshaft engines

According to the concept developed in [20], the actuating mechanism (AM) and TE were considered as a single whole: an invariable part of the system. This approach has proven itself in the synthesis of TE control algorithms for helicopters of civil aviation or transport aviation. For such control objects, the dynamic processes in the fuel system proceed much faster than in the engine; therefore, their influence on TE was simply neglected. But in TE, transient processes in the fuel and engine assembly occur almost simultaneously. This statement has been repeatedly confirmed by the results of full-scale tests [21]. On the basis of the foregoing, we single out the TE and AM directly into separate links – the fuel metering unit (FMU) and modify the structural diagram of the ACS shown in fig. 1 (fig. 4).

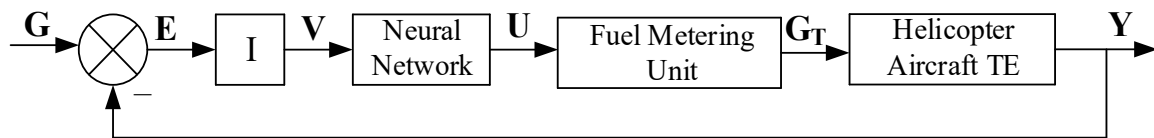


**Figure 4:** Structural diagram of a modified multidimensional ACS of helicopters aircraft TE with a divided control object on FMU and TE

When conducting a simple study of the operation of the ACS TE, which consists in various combinations of parameters for transfer functions for TE and FMU, it was found that the quality of control (accuracy, overshoot, stability margins) changes dramatically when switching from mode to mode. Thus, the task of analyzing the quality of control and synthesizing control algorithms for objects of this class becomes very relevant.

In this paper, the ACS of TE is studied and the quality of control is analyzed taking into account the dynamics of the FMU and TE. Consider the automatic control system of the gas turbine engine shown in fig. 4. The system consists of a comparison element (CE), a regulator, FMU and TE. The initial value of r.p.m. and gas temperature in front of the compressor turbine and the obtained values of the number of these parameters are received at the input of the CE, the inconsistency of the incoming parameters is formed at the output and the system error is formed –  $\zeta$  [20, 21]. The error is fed to the input of the controller, the signal  $u$  is generated at the output, which is fed to the input of the FMU, the signal of fuel consumption  $G_T$  is generated at the output, which is fed to the input of TE and, accordingly, the signal  $Y$  is generated, which is fed to the input of the CE. Taking into account that in the proposed ACS scheme of TE the control object was divided, it is advisable to introduce nonlinear models separately for the TE and FMU and simulate the operation of the system, taking into account the dynamics of its elements. In order to investigate the above-described ACS TE, it is also proposed to introduce mathematical models of the FMU and TE into the structure of the system in order to improve the quality of control of the entire system as a whole [20, 21].

On fig. 5 shows the ACS TE scheme developed in this work. In the logical block (LB) the input signals are analyzed as follows: a knowledge base is built on the basis of experimental data and conclusions. In relation to it, membership functions are formed for the input parameters of the LB, as well as output signals [22]. Having formed the necessary change, the LB sends response signals to the input of the comparison element, forming a control signal that is fed to the input of the FMU and its model. The LB receives two signals: the inconsistency of the FMU and TE models with the FMU and TE models – model error ( $\zeta_{mod}$ ) and the inconsistency of the FMU with the FMU model – FMU error ( $\zeta_{FMU}$ ). As practice shows, the TE error is small and is not taken into account in the course of the study.



For one channel, the GTE transfer function  $H_{TE}(p) = k_{TE} \cdot \frac{A(p)}{B(p)}$ , then  $\frac{1}{H_{TE}(p)} = \frac{1}{k_{TE}} \cdot \frac{B(p)}{A(p)}$ . If an open-loop transfer function  $W^*(p)$  is required:

$$W^*(p) = \frac{\Phi^*(p)}{1 - \Phi^*(p)} = \frac{k}{p \cdot C(p)}; \quad (8)$$

where  $\frac{k}{p}$  – determines system astatism, and  $\frac{1}{C(p)}$  – its inertia, then the transfer function of the control device will take the form:

$$W_{CD} = \frac{1}{k_{TE}} \cdot \frac{B(p)}{A(p)} \cdot \frac{k}{p \cdot C(p)}. \quad (9)$$

In the ACS of complex technical objects, professor Valery Petunin proposed the implementation of a common isodromic controller [23] with a transfer function:

$$W_{IC}(p) = \frac{k_{IC} \cdot (T_{IC} \cdot p + 1)}{p \cdot C(p)}; \quad (10)$$

where the boosting link  $(T_{IC} \cdot p + 1)$  corrects the inertia of TE and regulators of individual channels:

$$W_{MD} = \frac{1}{k_{TE_i}} \cdot \frac{B(p)}{A_i(p)} \cdot \frac{k}{k_{IC} \cdot (T_{IC} \cdot p + 1)}. \quad (11)$$

Mathematical description of the desired automatic control system.

The block diagram of the desired ACS of one channel is shown in fig. 7, where  $W^*(p)$  – transfer function of the desired open-loop system.

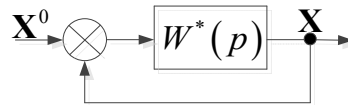


**Figure 7:** Structural diagram of the desired ACS

Then the transfer function of the closed desired system can be represented as:

$$\Phi^*(p) = \frac{W^*(p)}{1 + W^*(p)}. \quad (12)$$

According to (8),  $W^*(p) = \frac{\Phi^*(p)}{1 - \Phi^*(p)}$ , and if  $W^*(p) = \frac{k}{p \cdot C(p)}$ , then

$$\Phi^*(p) = \frac{k}{p \cdot C(p) + k}. \quad (13)$$

The inertia of the actuators must be taken into account in  $C(p)$ , if necessary, it can be adjusted. The transfer function of a closed system  $\Phi^*(p)$  should be close to the standard transfer function, taking into account the requirements for the quality of transient processes.

Synthesis of controlling channel for gas generator r.p.m.

For the fuel dosing circuit into the main combustion chamber by the speed channel, the transfer function of helicopter aircraft TE can be represented as:

$$H_{nGr}(p) = k_n \cdot \frac{A_n(p)}{B(p)}; \quad (14)$$

where the order of the polynomial  $A_n(p)$  is one less than the order of  $B(p)$  (table 1).

**Table 1**

Correspondence of polynomial order on the number of shafts of helicopters aircraft TE

Number of helicopters aircraft TE shafts	Polynomial order	
1	0	1
2	1	2

Transfer function of a one-shaft TE (for example, GTE-350) in terms of gas generator r.p.m. can be obtained according to [23] in the form:

$$H_{n_{Gr}}(p) = \frac{0,4}{0,5 \cdot p + 1}. \quad (15)$$

Then the transfer function of the control device for gas generator r.p.m. channel is represented as:

$$W_{CDn}(p) = \frac{1}{k_n} \cdot \frac{B(p)}{A_n(p)} \cdot \frac{k}{p \cdot C(p)}. \quad (16)$$

If the transfer function of the desired system  $W^*(p) = \frac{3}{p \cdot (0,02 \cdot p + 1)}$  and the transfer function of the general isodromic controller  $W_{IC}(p) = \frac{3 \cdot (0,56 \cdot p + 1)}{p \cdot (0,02 \cdot p + 1)}$  [23, 25], then the transfer function of the controller over the channel of gas generator r.p.m.:

$$W_n(p) = W_1(p) = \frac{1}{0,4} = 2,5. \quad (17)$$

For emergency operation, the transfer function of two-shaft TE (for example, TV3-117) in terms of gas generator r.p.m. can be obtained in accordance with [23, 25]:

$$H_{n_{rcGr}}(p) = \frac{0,186 \cdot p + 0,875}{0,133 \cdot p^2 + 0,94 \cdot p + 1}. \quad (18)$$

Then the transfer function of the control device for gas generator r.p.m. channel is:

$$W_{CDn_{rc}}(p) = \frac{1}{k_{n_{rc}}} \cdot \frac{B(p)}{A_{n_{rc}}(p)} \cdot \frac{k}{p \cdot C(p)}. \quad (19)$$

If the transfer function of the desired system  $W^*(p) = \frac{3}{p \cdot (0,02 \cdot p + 1)}$  and the transfer function of the general isodromic controller  $W_{IC}(p) = \frac{3 \cdot (0,766 \cdot p + 1)}{p \cdot (0,02 \cdot p + 1)}$  [23, 25], then the transfer function of the controller over the channel of gas generator r.p.m.:

$$W_{n_{rc}}(p) = W_1(p) = \frac{1}{0,766} \cdot \frac{0,175 \cdot p + 1}{0,210 \cdot p + 1} = \frac{0,229 \cdot p + 1,306}{0,210 \cdot p + 1}. \quad (20)$$

Synthesis of the gas temperature control channel before the compressor turbine.

For the fuel dosing circuit into the combustion chamber by the gas temperature channel before the compressor turbine, the transfer function of helicopter aircraft TE can be represented as:

$$H_{T_G^*Gr}(p) = k_{T_G^*} \cdot \frac{A_{T_G^*Gr}(p)}{B(p)}; \quad (21)$$

where  $A_{T_G^*Gr}(p)$  and  $B(p)$  are polynomials of the same order (table 2).

**Table 2**

Correspondence of polynomial order on the number of shafts of helicopters aircraft TE

Number of helicopters aircraft TE shafts	Polynomial order	
1	1	1
2	2	2

For emergency operation, the transfer function of a one-shaft TE in terms of gas temperature in front of the compressor turbine can be obtained according to [23, 25]:

$$H_{T_G^*Gr}(p) = 0,35 \cdot \frac{0,829 \cdot p}{0,56 \cdot p + 1} = \frac{0,29 \cdot p}{0,56 \cdot p + 1}. \quad (22)$$

Then the transfer function of the control device for the gas temperature channel before the compressor turbine has the form:

$$H_{ICT_G^*}(p) = \frac{1}{k_{T_G^*}} \cdot \frac{B(p)}{A_{T_G^* G_T}(p)} \cdot \frac{k}{p \cdot C(p)}. \quad (23)$$

If the transfer function of the desired system  $W^*(p) = \frac{3}{p \cdot (0,02 \cdot p + 1)}$  and the transfer function of the general isodromic controller  $W_{IC}(p) = \frac{3 \cdot (0,56 \cdot p + 1)}{p \cdot (0,02 \cdot p + 1)}$  [23, 25], then transfer function of the controller through the gas temperature channel before the compressor turbine will look like:

$$W_{T_G^*}^*(p) = W_2(p) = \frac{1}{0,35} \cdot \frac{1}{0,829 \cdot p + 1} = \frac{2,857}{0,829 \cdot p + 1}. \quad (24)$$

For emergency operation, the transfer function of a two-shaft TE in terms of gas temperature in front of the compressor turbine can be obtained in accordance with [13, 15]:

$$H_{T_G^* G_T}(p) = 0,333 \cdot \frac{0,064 \cdot p^2 + 0,667 \cdot p + 1}{0,133 \cdot p^2 + 0,94 \cdot p + 1} = \frac{0,021 \cdot p^2 + 0,222 \cdot p + 0,333}{(0,766 \cdot p + 1) \cdot (0,174 \cdot p + 1)}. \quad (25)$$

Then the transfer function of the control device for the gas temperature channel before the compressor turbine looks like this:

$$H_{ICT_G^*}(p) = \frac{1}{k_{T_G^*}} \cdot \frac{B(p)}{A_{T_G^* G_T}(p)} \cdot \frac{k}{p \cdot C(p)}. \quad (26)$$

If the transfer function of the desired system  $W^*(p) = \frac{3}{p \cdot (0,02 \cdot p + 1)}$  and the transfer function of the general isodromic controller  $W_{IC}(p) = \frac{3 \cdot (0,56 \cdot p + 1)}{p \cdot (0,02 \cdot p + 1)}$  [23, 25], then transfer function of the controller through the gas temperature channel before the compressor turbine will look like:

$$W_{T_G^*}^*(p) = W_2(p) = \frac{1}{0,333} \cdot \frac{0,174 \cdot p + 1}{0,064 \cdot p^2 + 0,667 \cdot p + 1} = \frac{0,522 \cdot p + 3}{0,064 \cdot p^2 + 0,667 \cdot p + 1}. \quad (27)$$

The principles of construction of fast-response GTE gas temperature meters were studied in [17].  
Synthesis of cross-links of control channels.

According to [23], it is assumed that  $W_{K1}(p)$  and  $W_{K2}(p)$  – transfer functions of corrective links, the results of the synthesis of which are given in [16], which have the form:

$$W_{K1}(p) = \frac{W_1(p) - 1}{W_2(p)}; \quad W_{K2}(p) = \frac{1 - W_2(p)}{W_2(p)}. \quad (28)$$

Then the expressions for the transfer functions for these links look like this:

1. For a one-shaft TE:

$$W_{K1}(p) = 0,428 \cdot (0,829 \cdot p + 1) = 0,355 \cdot p + 0,428; \quad W_{K2}(p) = 0,35 \cdot (0,829 \cdot p - 1,857) = 0,29 \cdot p - 0,65.$$

2. For a two-shaft TE:

$$W_{K1}(p) = \frac{-0,0018 \cdot p + 0,0517}{0,206 \cdot p + 1} \cdot \frac{0,064 \cdot p^2 + 0,667 \cdot p + 1}{0,174 \cdot p + 1}; \quad W_{K2}(p) = 0,333 \cdot \frac{0,064 \cdot p^2 + 0,145 \cdot p - 2}{0,174 \cdot p + 1}.$$

According to [23], the corrective element  $W_1(p)$  of the ACS control channel is permanently switched on, and the corrective element  $W_2(p)$  is implemented when the limitation channel is turned on by parallel connection to  $W_1(p)$  of a differential dynamic link with a transfer function according to the output logical signal of the selector  $L$ :

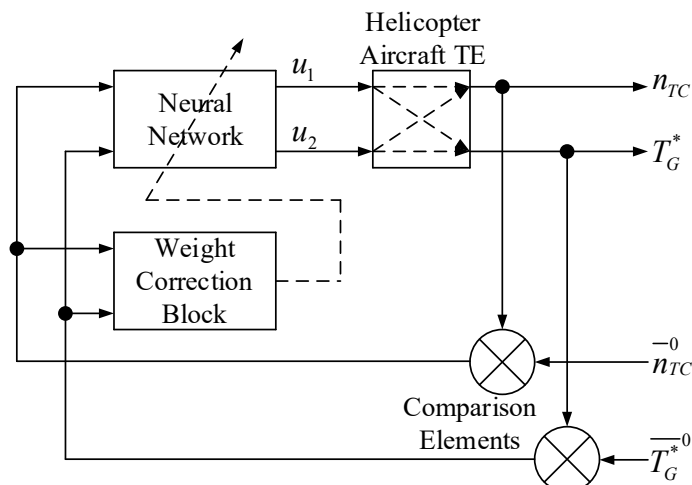
$$W_{\Delta}(p) = W_1(p) - W_2(p). \quad (29)$$

1. For a one-shaft TE:  $W_{\Delta}(p) = \frac{1,842 \cdot p - 0,653}{0,829 \cdot p + 1}$ .

2. For a two-shaft TE:  $W_{\Delta}(p) = \frac{0,174 \cdot p + 1}{0,206 \cdot p + 1} \cdot \frac{0,0739 \cdot p^2 + 0,152 \cdot p - 1,845}{0,064 \cdot p^2 + 0,667 \cdot p + 1}$ .

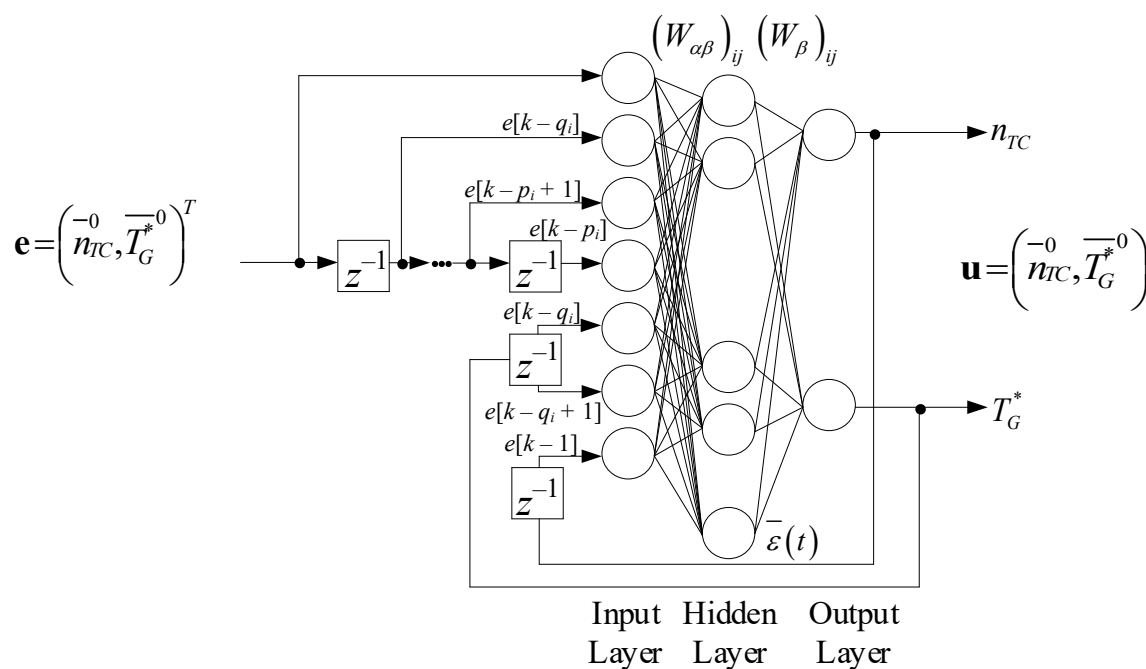
## 6. Development of a neural network for implementation of multidimensional automatic control system for helicopters turboshaft engines

Fig. 8 shows a block diagram of the proposed self-adjusting neural network control system for helicopters aircraft TE with interconnected coordinates.



**Figure 8:** Proposed neural network control system for helicopters aircraft TE with interconnected coordinates

The control error vector  $\mathbf{e} = [e_1, e_2, \dots, e_n]^T$  after the comparison elements is fed to the input of the neural network and the weight correction block, in which, depending on the signal  $\mathbf{e}(t)$ , at each discrete time  $t$ , the weight coefficients of the neural network are adjusted. The vector of signals  $\mathbf{u} = [u_1, u_2, \dots, u_n]^T$  from neural network output is the control one and is fed to the input of the control object (helicopter aircraft TE). The neural network for controlling aviation gas turbine engines of helicopters as multiply connected objects is a multilayer neural network with one intermediate layer containing  $N_0$  neurons in the input layer and  $N_2$  neurons in the output layer, with  $N_2 = N_0 = n$ . The network is characterized by the number of neurons  $N_1$  in the inner layer (layer 1) [28]. The structure of a multilayer neural network is shown in fig. 9.



**Figure 9:** Structure of the neural network of a self-tuning system regulation

The input layer (layer 0) consists of nodes – signal receivers  $e_i$  ( $i = \overline{1, n}$ ), the output layer – of neurons – signal sources  $u_i$  ( $i = \overline{1, n}$ ). Signals  $e_i$  are fed to the input of the neural network of a discrete moment of time  $t$  ( $t = 0, 1, 2, \dots$ ), which are converted by the network into control signals  $u_i$ . The discrete time  $t$  is related to the continuous time  $\Theta$  as follows:  $\Theta = \delta \cdot t$ , where  $\delta$  – quantization step. Each  $i$  neuron of the  $l$ -th layer ( $l = \overline{1, 2}$ ) transforms the input vector into the original scalar value. At the first stage, the superposition of the input signals of the neuron is calculated:

$$z_i^l = \sum_{j=1}^{N_{l-1}} w_{ij}^l \cdot o_j^{l-1} - g_i^l; \quad (30)$$

where  $w_{ij}^l$  – weight coefficient, which is an adjustable parameter and characterizes the connection of the  $j$ -th neuron ( $l-1$ ) of the layer with the  $i$ -th neuron of the  $l$ -th layer;  $g_i^l$  – shift amount.

Assuming that  $w_{i0}^l = -g_i^l$  and  $o_0^{l-1} = 1$ , expression (30) is rewritten as:

$$z_i^l = \sum_{j=1}^{N_{l-1}} w_{ij}^l \cdot o_j^{l-1}. \quad (31)$$

Next, the value of  $z$  is converted to the initial value of the neuron:

$$o_i^l = f(z_i^l). \quad (32)$$

The nonlinear transformation (32) is defined by an activation function, often defined as a sigmoid function:

$$f(z) = \frac{1}{1 + e^{-z}}. \quad (33)$$

An important property of this function is the simplicity of determining the derivative of this function, i.e.

$$f'(z) = f(z) \cdot (1 - f(z)). \quad (34)$$

With the accepted notation, the mathematical description of the neural network is written using the system of equations:

$$\begin{cases} u_j(t) = o_j^2; j = \overline{1, n}; \\ o_i^l = f(z_i^l); i = \overline{1, N_l}; l = \overline{1, 2}; \\ z_i^l = \sum_{j=1}^{N_{l-1}} w_{ij}^l \cdot o_j^{l-1}; i = \overline{1, N_l}; l = \overline{1, 2}; \\ o_j^0 = e_j(t); j = \overline{1, n}; \\ o_0^0 = o_0^1 = 1. \end{cases} \quad (35)$$

During the operation of a self-adjusting neural network control system, the system settings – the weight coefficients of the neural network change in such a way that the value  $E = \|\mathbf{e}\| \rightarrow 0$ , while the value of  $E = \frac{1}{2} \cdot \sum_{i=1}^n \alpha_i \cdot e_i^2$ , where  $\alpha_i$  – coefficients that determine the weight of each control channel of the total error  $E$ , is taken as the norm of the vector  $E$ .

Correction of neural network weight coefficients  $w_{ij}^l$  (training of the neural network) is carried out in the block for correcting the weight coefficients by backpropagation error method [29, 30]. The main calculated ratios in this case have the form:

$$w_{ij}^l(t) = w_{ij}^l(t-1) - \gamma \cdot \delta \cdot \frac{\partial E}{\partial w_{ij}^l}. \quad (36)$$

For the weight coefficients of the neuron of the original layer (layer 2), the values  $\frac{\partial E}{\partial w_{ij}^{(2)}}$  are determined according to the expression:

$$\frac{\partial E}{\partial w_{ij}^{(2)}} = \sum_{k=1}^n \left( \alpha_k \cdot e_k \cdot \frac{\partial y_k}{\partial u_i} \right) \cdot f'(z_i^{(2)}) \cdot o_j^{(1)}; \quad k = \overline{1, n}; \quad i = \overline{1, n}; \quad j = \overline{1, N_1}; \quad (37)$$

where  $e_k$  – control error for the  $k$ -th initial variable;  $\alpha_k$  – weight coefficient for the  $k$ -th output variable;  $\frac{\partial y_k}{\partial u_i}$  – derivative of the  $k$ -th output variable of the object with respect to the  $i$ -th input action;

$f'(z_i^{(2)})$  – derivative of the activation function for the  $i$ -th neuron of the second (initial) layer;  $o_j^{(1)}$  – initial value of the  $j$ -th neuron of the first layer.

For the inner layer (layer 1), the values  $\frac{\partial E}{\partial w_{ij}^{(1)}}$  are determined by the scalar product:

$$\frac{\partial E}{\partial w_{ij}^{(1)}} = \left( \bar{\mathbf{a}} \times \mathbf{e}, \mathbf{Y}_u \times \mathbf{U}_{w_{ij}^{(1)}} \right); \quad i = \overline{1, N_1}; \quad j = \overline{0, n}; \quad (38)$$

where  $\bar{\mathbf{a}}$  – matrix of weight coefficients of variable adjustments;  $\mathbf{e}$  – adjustment error vector;  $\mathbf{Y}_u$  – matrix of derivative variables of regulation with respect to incoming control actions;  $\mathbf{U}_{w_{ij}^{(1)}}$  – vector of derivatives of the output signals of the neural network by the weight  $w_{ij}^{(1)}$  of the layer 1 neuron;  $\bar{\mathbf{a}} \times \mathbf{e}$  – vector product of matrix  $\bar{\mathbf{a}}$  and vector  $\mathbf{e}$ ;  $\mathbf{Y}_u \times \mathbf{U}_{w_{ij}^{(1)}}$  – vector product of matrix  $\mathbf{Y}_u$  and vector  $\mathbf{U}_{w_{ij}^{(1)}}$ .

The presented vectors and matrices look like this:

$$\bar{\mathbf{a}} = \begin{pmatrix} \alpha_1 & 0 & \dots & 0 \\ 0 & \alpha_2 & \dots & 0 \\ M & M & \dots & M \\ 0 & 0 & \dots & \alpha_n \end{pmatrix}; \quad \mathbf{e} = \begin{pmatrix} e_1 \\ e_2 \\ M \\ e_n \end{pmatrix}; \quad \mathbf{Y}_u = \begin{pmatrix} \frac{\partial y_1}{\partial u_1} & \frac{\partial y_1}{\partial u_2} & \dots & \frac{\partial y_1}{\partial u_n} \\ \frac{\partial y_2}{\partial u_1} & \frac{\partial y_2}{\partial u_2} & \dots & \frac{\partial y_2}{\partial u_n} \\ M & M & \dots & M \\ \frac{\partial y_n}{\partial u_1} & \frac{\partial y_n}{\partial u_2} & \dots & \frac{\partial y_n}{\partial u_n} \end{pmatrix}; \quad \mathbf{U}_{w_{ij}^{(1)}} = \begin{pmatrix} \frac{\partial u_1}{\partial w_{ij}^{(2)}} \\ \frac{\partial u_2}{\partial w_{ij}^{(2)}} \\ M \\ \frac{\partial u_n}{\partial w_{ij}^{(2)}} \end{pmatrix}.$$

With the machine implementation of the presented learning algorithm, the matrix  $\mathbf{Y}_u$  will be a matrix consisting of a set of zeros and ones, and the ones will be equal to the element corresponding to the main (direct) control channels. For an object with  $n$  inputs and outputs, the  $\mathbf{Y}_u$  matrix might look like this:

$$\mathbf{Y}_u = \begin{pmatrix} 1 & 0 & \dots & 0 \\ 0 & 1 & \dots & 0 \\ M & M & \dots & M \\ 0 & 0 & \dots & 1 \end{pmatrix}. \quad (39)$$

The vector  $\mathbf{U}_{w_{ij}^{(1)}}$  elements  $\frac{\partial u_k}{\partial w_{ij}^{(1)}}$  are determined according to the expression:

$$\frac{\partial u_k}{\partial w_{ij}^{(1)}} = f'(z_k^{(2)}) \cdot w_{ki}^{(2)} \cdot f'(z_i^{(1)}) \cdot o_j^{(0)}; \quad k = \overline{1, n}; \quad i = \overline{1, N_1}; \quad j = \overline{0, n}. \quad (40)$$

Before the start of the self-adjusting control system, the system parameters are set: in the weight correction block – weight coefficients setting parameter  $\gamma$ , in the neural network block – number of neurons in the inner layer  $N_1$  and the weight coefficients  $w_{ij}^{(l)}$  of the neurons of layers 1 and 2. Coefficients  $w_{ij}^{(l)}$  are selected by a random sensor  $[-1, 1]$  according to the uniform distribution law.

## 7. Simulation studies of the neural network control system of helicopters aircraft turboshaft engines

TV3-117 aircraft TE, which is part of the power plant of Mi-8MTV helicopter with two inputs ( $n_{TC}$ ,  $T_G^*$ ), one output ( $\overline{G_T}$ ) and the presence of significant cross-links (fig. 10) [17–19], was used as research object.

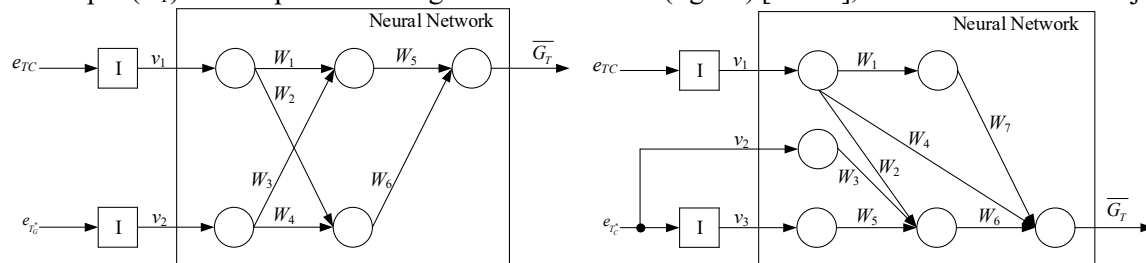


**Figure 10:** Structural diagram of control object (TV3-117 aircraft TE)

On fig. 11, the diagrams of transient processes in the system during testing set the impact without preliminary self-tuning according to the model (curves 1, 2) and with preliminary self-tuning (curves 3, 4). Quite often, at the initial stage of self-adjustment (when the neuroregulator is first switched on in the control loop), large outliers of controlled values from the set values are observed (fig. 11, curve 1). This is due to the fact that when the neuroregulator is turned on, the weight coefficients of the neural network are initialized randomly. In this case, there is a possibility of organizing positive feedbacks, which are the source of too large deviations of controlled values at the initial stage of self-tuning. The occurrence of such a situation can lead to emergency situations on the helicopter.

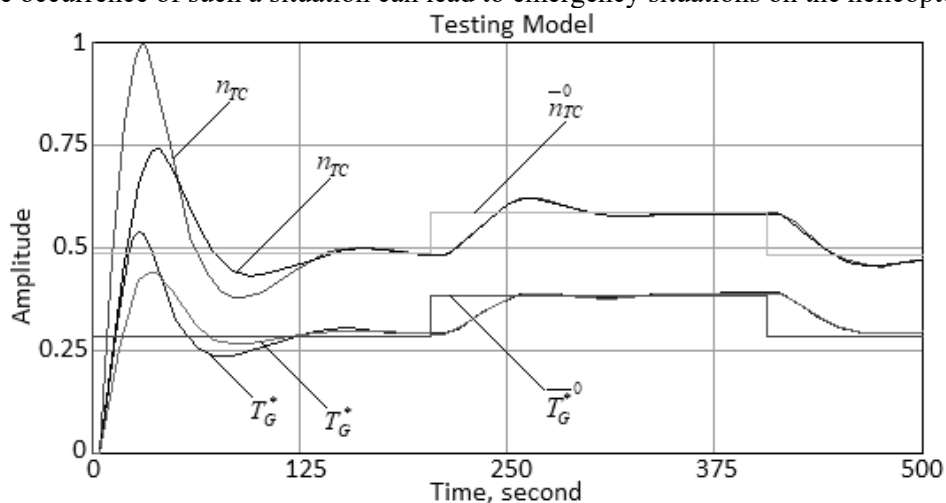


**Figure 11:** Influence of preliminary self-tuning according to the model on the quality of the control process

The availability of a priori information about helicopter aircraft TE, its dynamic and static characteristics will significantly reduce the deviation of controlled values in the process of self-tuning. This is ensured by the fact that at the previous stage the self-tuning of the system is carried out according to the approximate model of the gas turbine engine. Then there is a switch to work with the control object (helicopter aircraft TE), the channels of which can be described by aperiodic links of the first order with a delay. The parameters of TE model are determined approximately. An error in estimating the parameters within  $\pm 100\%$  has little effect on subsequent self-tuning results, with the highest sensitivity observed behind the gain. The parameters of the control system built using a neural network are the neurons number in the hidden layer  $N_1$  and the correction parameter of neural network weights coefficient  $\gamma$ . On fig. 12 show the influence of the tuning parameters  $N_1$  and  $\gamma$  on the quality of the regulation process. With an increase in the values of the parameters  $N_1$  and  $\gamma$ , the speed of the system increases, but the values of the overshoot and dynamic error also increase, and the value of the degree of extinction of transient processes decreases. With a significant increase in the values of the tuning parameters, undamped oscillations and instability of the control process may occur.

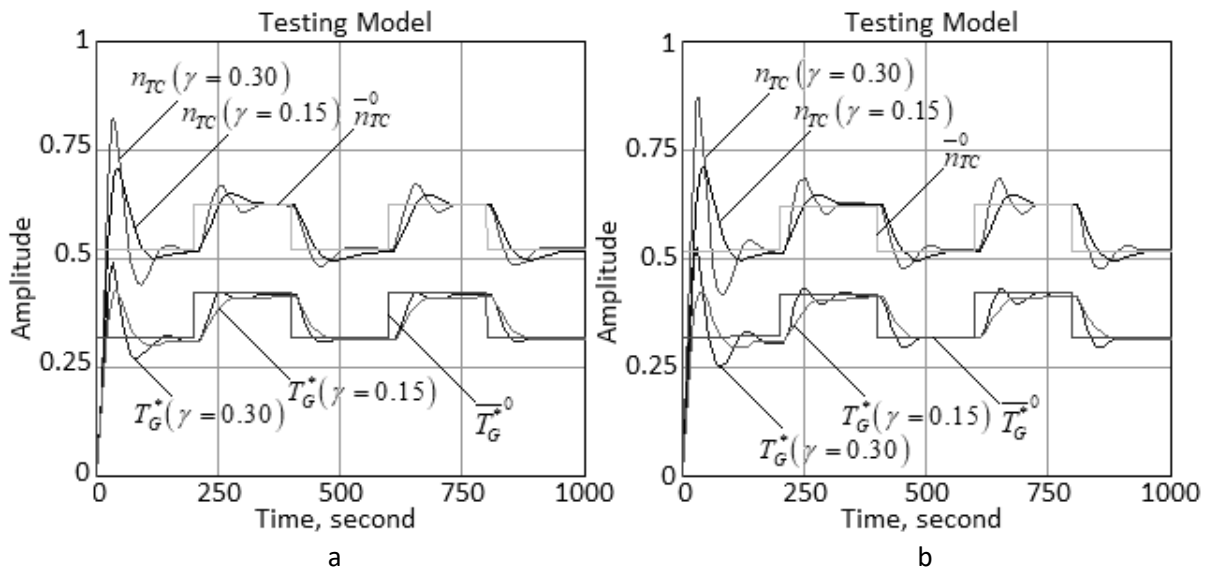


**Figure 12:** Influence diagrams: a – number of neurons  $N_1$  in the intermediate layer on the quality of the regulation process; b – weight correction factor for the quality of the control process

Neural network control system for helicopters aircraft TE works out quite well both external disturbing influences (fig. 13, a), and setting influences (fig. 13, b), as well as antiphase setting actions (fig. 13, c).

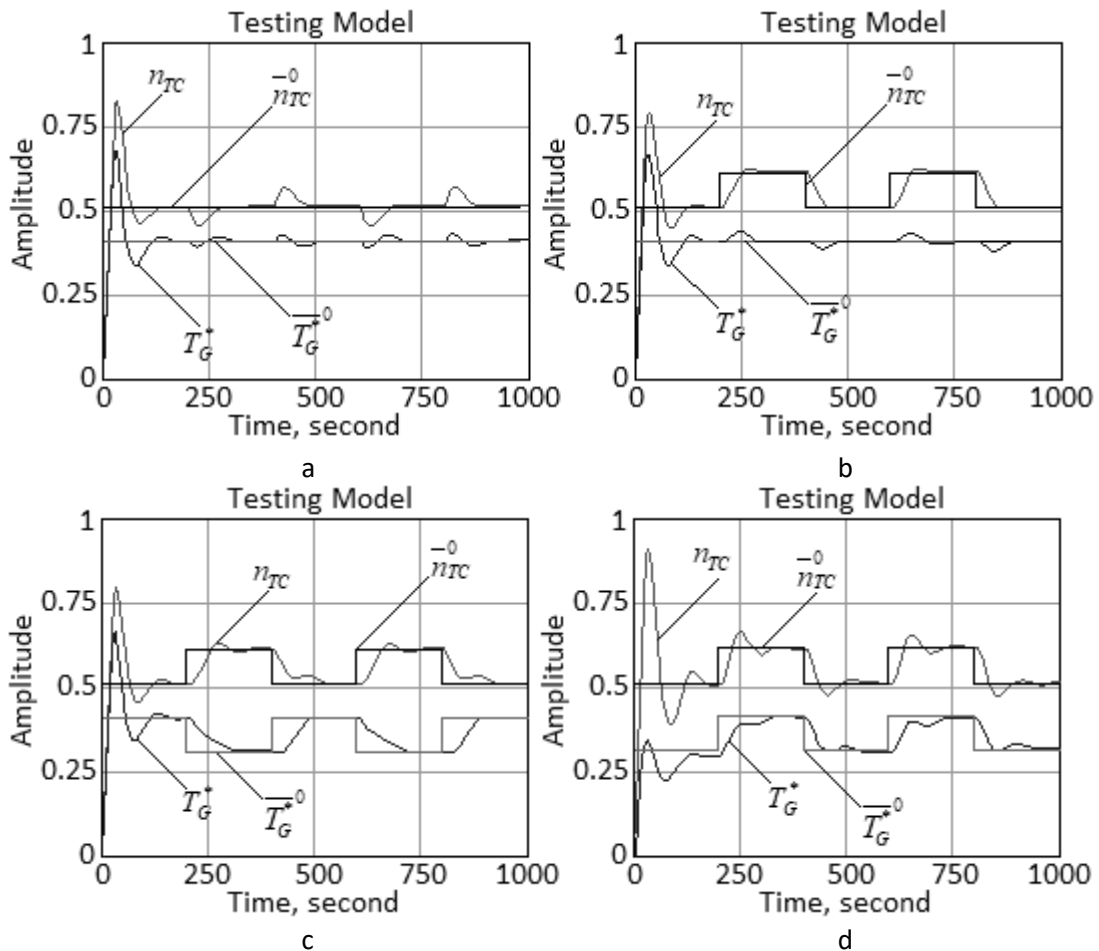


**Figure 13:** Process diagrams: a – square wave perturbations; b – one master influence; c – two setting influences going out of phase; d – setting influences when changing the gain coefficients of TV3-117 aircraft TE channels

In a neural network control system, as in classical systems, cross channels have a significant impact on the quality of regulation. With a decrease in the influence of cross-links (a decrease in the coupling coefficient  $\frac{K_{12}K_{21}}{K_{11}K_{22}}$ ), the quality of regulation improves significantly. An important property

of a neural network control system is the possibility of its effective adaptation to changes in the properties of the control object. In the course of simulation studies, the influence of changing the properties of the control object on the quality of the regulation process in the system was considered. On fig. 13, d shows the transient process in the system during the development of two setting actions and in the form of square waves. At the same time, during the process, the gain factors along the channels of the control object changed: the coefficients  $K_{11}$  and  $K_{22}$  linearly decreased from 2.0 to 1.0 and from 1.5 to 1.0, respectively, and the coefficients  $K_{12}$  and  $K_{21}$  linearly increased from 0.3 to 0.5 and from 0.4 to 0.6, respectively. As can be seen from fig. 13, d, the high quality of regulation is maintained with a sufficiently large variation (30...100 %) of the gains of the object's channels, that is, the neural network control system adapts to changes in the gains of the object's channels.

The proposed neural network automatic control system of helicopters aircraft TE adapts well to changes in time constants and delays – changing them even by two or three times does not have a significant effect on changing the quality of regulation in the system.

## 8. Neural network training results

The input data for training the neural network is massive of  $n_{TC}$  and  $T_G^*$  parameters recorded on board the helicopter. *Accuracy*, *Precision*, *Recall*, *F*-measure metrics are used to assess the quality of neural network training. *Precision* can be interpreted as the proportion of parameters that the neural network called positive and at the same time are really positive, and *Recall* shows what proportion of the parameters of the positive class of all objects of the positive class was found by the algorithm [31]. The results of training the neural network according to the *Accuracy* and *Loss* indicators are shown in fig. 14. As can be seen from fig. 14, the *Accuracy* indicator approaches one, and *Loss* indicator – tends to zero, which indicates the high accuracy of the model and its minimal error.

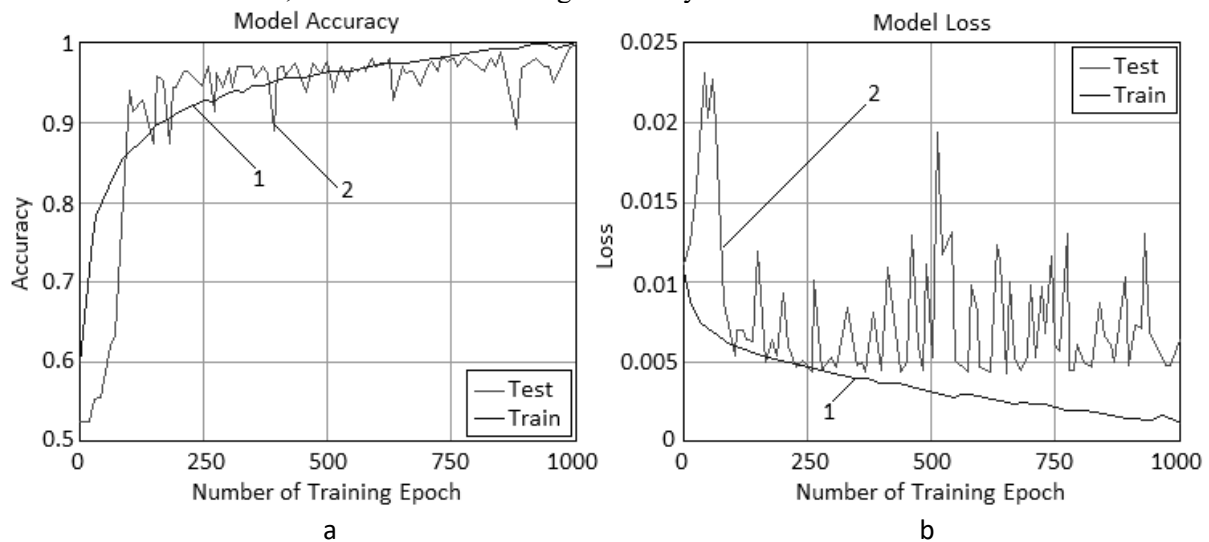


**Figure 14:** Neural network classifier training results (1 – test; 2 – train): a – *Accuracy* indicator; b – *Loss* indicator

## 9. Results and discussion

To assess the quality of ACS helicopters aircraft TE control, we introduce the following requirements:

- amplitude stability margin: not less than 20 dB;

- phase stability margin: from 35 to 80°;
- overshoot: no more than 5%;
- static error: no more than  $\pm 5\%$  ( $\pm 0.05$ );
- regulation time: no more than 5 s.

When modeling the system (fig. 15, b), it was found that only with the values of the time constant ( $T$ ) for the transfer functions of the FMU and TE:  $T = 0.7$  s,  $T = 0.5$  s,  $T = 1$  s and transfer coefficient  $k = 1$  the system works optimally, meeting the requirements of control quality and system stability. This indicates that the system changes parameters when operating in other modes, the quality of control of which may not meet the requirements. Therefore, we will take for ACS helicopters aircraft TE value of the time constant  $T = 0.7$  s and the gain  $k = 1$ , and we will consider the system ideal, taken as a standard in the forthcoming study. Using the experimental data obtained during various passages of the routes, the points associated with the change in altitude and flight speed were selected: for a time of 50, 200, 500 s. According to [32], using the experimental data at the selected points, the values of the time constant and gain for the FMU and TE were obtained. When modeling in the ACS scheme of helicopters aircraft TE, the models of FMU and TE changed alternately with the obtained experimental parameters of the wind turbine and gas turbine engine, which made it possible to analyze the system according to the requirements described above. In the future, we will use the simulation time of 50 s, since it will be enough for the study.

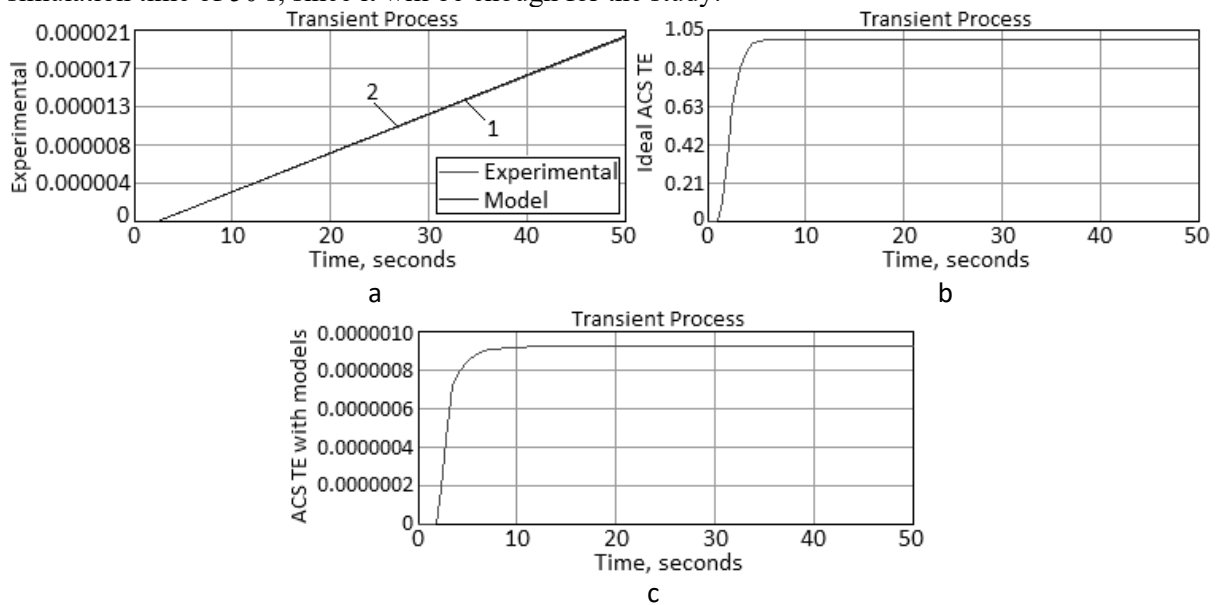


**Figure 15:** Results of the simulation of helicopters aircraft turboshaft engines automatic control system during the simulation time of 50 s: a – transient process of helicopters aircraft turboshaft engines automatic control system with experimental data (1), helicopters aircraft turboshaft engines automatic control system with models of FMU and TE (2); b – ideal ACS TE; c – ACS TE with models

The results of simulation of ACS TE for 50 s are shown in fig. 15. Modeling of the system was carried out in three stages: for an ideal scheme, with the parameters used in the design of helicopters aircraft turboshaft engines automatic control system, as well as for the system with experimental data and the system using the above approach with mathematical models of FMU and TE to adjust the operation of the entire system. As can be seen from the fig. 15, the transient process with ideal transfer function parameters for FMU and TE is established during the regulation time, which is 5 s; the system with experimental values is quite inertial and does not meet the requirements of control quality and stability, to adjust the helicopters aircraft turboshaft engines automatic control system, mathematical models of FMU and TE were introduced, which reduced the control time and began to meet the requirements. As can be seen from fig. 15, c, the transient process of the proposed ACS TE is inferior in quality: the value does not reach unity. Thus, in order to increase the accuracy of the transient process, it is proposed to introduce an LB based on fuzzy logic, the knowledge base and membership functions of which for input and output parameters will correspond to the graph of the dependence of errors on the control signal (fig. 16).

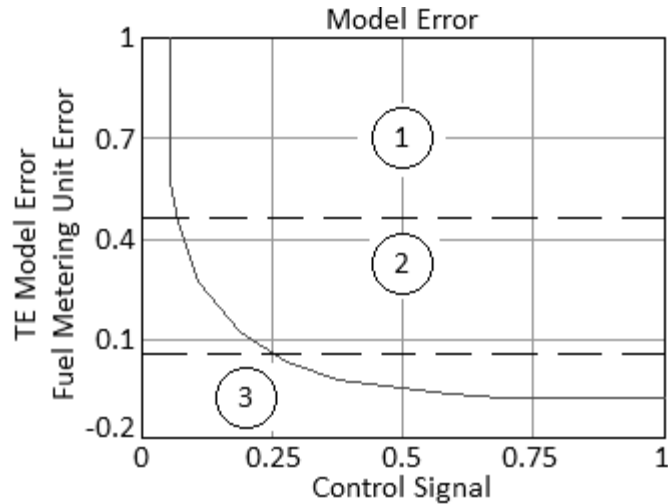


**Figure 16:** Dependence of model and ADT errors ( $\xi_{mod}$ ,  $\xi_{FMU}$ ) on control signal divided into zones: 1 – minimum, 2 – average, 3 – maximum

To ensure an acceptable nature of the transition process of the proposed ACS TE, it is proposed to introduce one more regulator: an integrating link. Experimental modeling showed that for the integrator the value of the gain ( $k$ ) equal to 150 became sufficient to increase the quality of the output parameters. On fig. 17 shows such a transient process, and several points are plotted on the graph, characterizing the ideal process. Such a parametric and structural change made it possible to qualitatively change the output parameters of the system with experimental data and approach the ideal parameters chosen in the article.

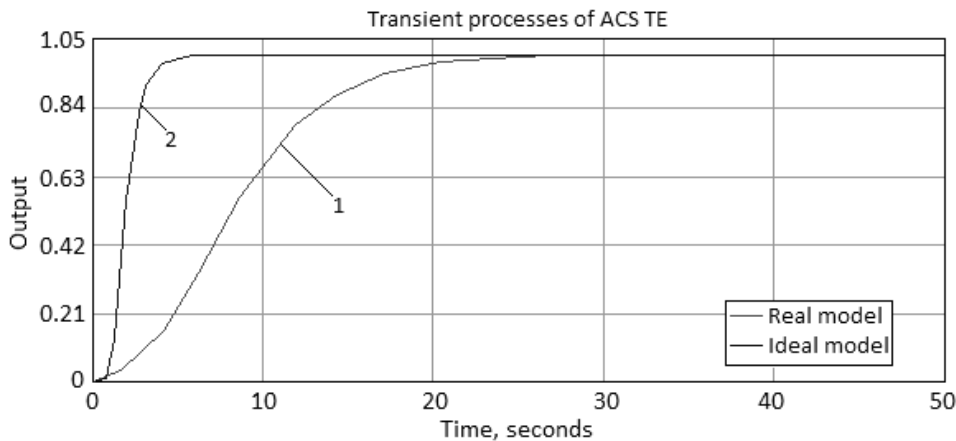


**Figure 17:** Transient processes of ACS TE with models and introduction of an integrator into the structure (1), ideal TE (2)

In [17, 18], the modeling of transient processes in steady-state operating modes (for nominal and emergency modes) was carried out using a multi-mode neural network controller based on a perceptron. In this paper, a similar study was carried out using the developed ACS TE based on a self-tuning neural network control system. Input data similar to [7, 8] are given in table 3.

**Table 3**

Input data of TV3-117 aircraft engine operating modes

TV3-117 aircraft engine operating modes	$n_{TC}$	$T_G^*$	$G_T$
$M_1$ (Nominal mode)	0.709	0.769	0.096
$M_2$ (Emergency mode)	1.092	1.087	0.334

Fig. 18 shows the results of modeling the automatic control system for TV3-117 gas turbine engine based on a self-adjusting neural network control system, from which it follows that the use of

the developed automatic control system increases the accuracy of modeling transient processes in the gas turbine engine control system, the graphs of which are close to the standard.

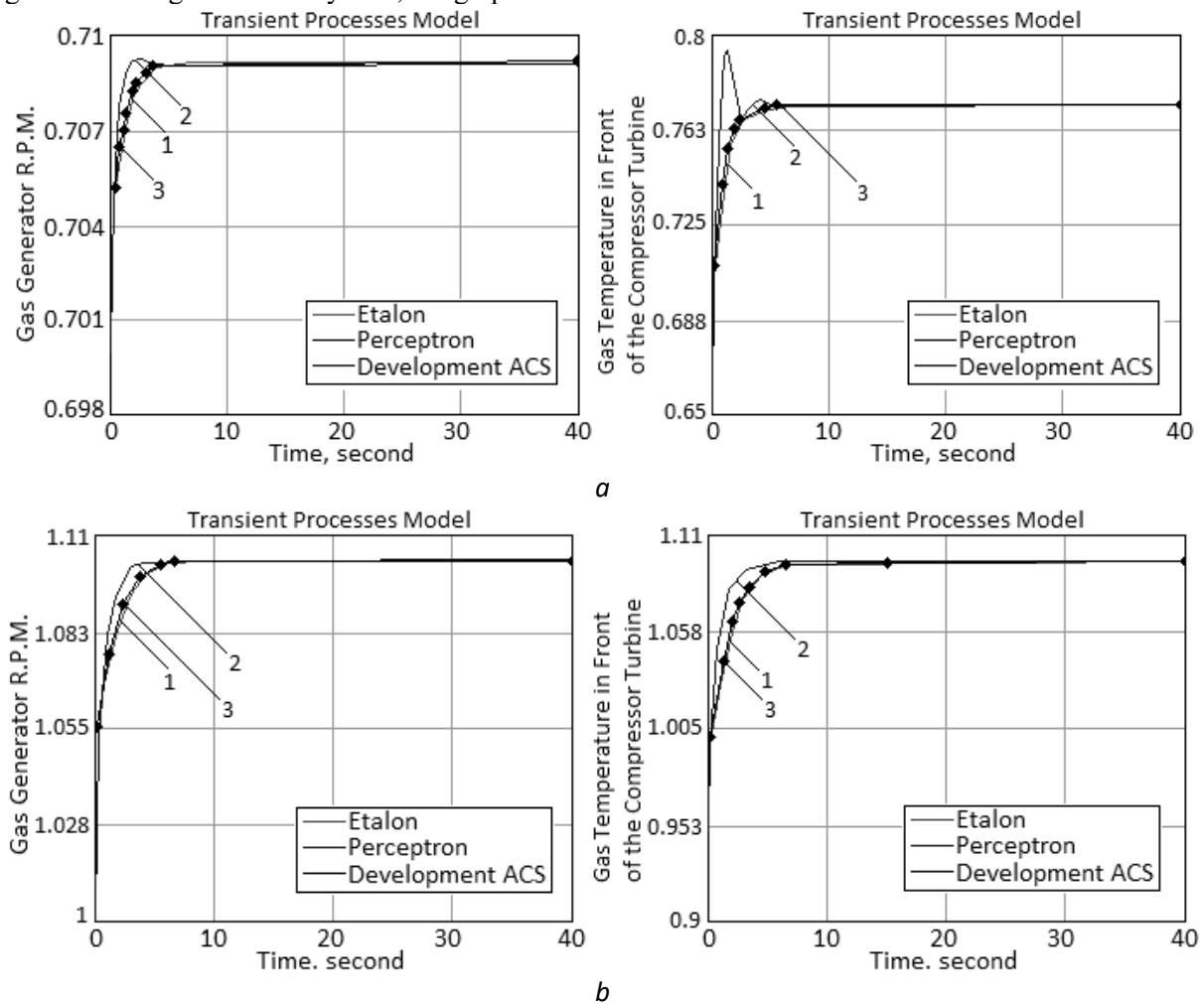


**Figure 18:** Results of modeling the automatic control system of TV3-117 aircraft engine: a – mode  $M_1$ ; b – mode  $M_2$ ; 1 – reference model; 2 – model with a multi-mode neural network controller based on perceptron; 3 – model with self-tuning neural network control system

## 10. Conclusions

The automatic control system of helicopters aircraft engines has been improved, in which the division of the control object into actuating mechanism and gas turbine engines makes it possible to take into account the dynamics of the executive part of the system and the engine, it becomes possible to use the mismatch between parts of the structural diagram of the automatic control system, thereby increasing the reliability and stability of the system in various modes.

The method for constructing a mathematical model of the automatic control system for helicopters aircraft engines, based on the selector of control channels according to the engine's thermogasdynamic parameters, was further developed by modifying the transfer functions, which made it possible to adapt the developed automatic control system for helicopters aircraft engines to a change in time constants and delays, namely, changing them even by two or three times does not have a significant effect on changing the quality of regulation in the system.

The self-adjusting neural network control system for multiply connected dynamic objects was further developed, the adaptation of which as a modified neural network controller of helicopters aircraft engines (by introducing an integrator into the system structure) made it possible to bring the graph of the real transient process in the engine closer to the ideal one, thereby increasing the reliability and stability of the system at various modes. The intelligent approach made it possible to

form a logical block, which qualitatively improved the output parameters of the system and made it possible to approach the ideal ones with a sufficient degree of accuracy.

## 11. References

- [1] S. N. Vassilyev, A. Yu. Kelina, Y. I. Kudinov, F. F. Pashchenko, Intelligent Control Systems, *Procedia Computer Science*, vol. 103 (2017) 623–628. doi: 10.1016/j.procs.2017.01.088
- [2] S. Pang, Q. Li, B. Ni, Improved nonlinear MPC for aircraft gas turbine engine based on semi-alternative optimization strategy, *Aerospace Science and Technology*, vol. 118 (2021), 106983. doi: 10.1016/j.ast.2021.106983
- [3] I. A. Krivosheev, K. E. Rozhkov, N. B. Simonov, Complex Diagnostic Index for Technical Condition Assessment for GTE, *Procedia Engineering*, vol. 206 (2017) 176–181. doi: 10.1016/j.proeng.2017.10.456
- [4] E. L. Ntantis, Diagnostic methods for an aircraft engine performance, *Journal of Engineering Science and Technology*, vol. 8, no. 4 (2015) 64–72. doi: 10.25103/jestr.084.10
- [5] S. Hosseinimaab, A. Tousei, A new approach to off-design performance analysis of gas turbine engines and its application, *Energy Conversion and Management*, vol. 243 (2021), 114411. doi: 10.1016/j.enconman.2021.114411
- [6] G. Dong, Y. Li, S. Sui, Fault detection and fuzzy tolerant control for complex stochastic multivariable nonlinear systems, *Neurocomputing*, vol. 275 (2018) 2392–2400. doi: 10.1007/s00500-019-04618-8
- [7] C. Rodriguez, J. Viola, Y. Q. Chen, Data-driven modelling for a high order multivariable thermal system and control, *IFAC-PapersOnLine*, vol. 54, issue 20 (2021) 753–758. doi: 10.1016/j.ifacol.2021.11.262
- [8] G.-Q. Zeng, X.-Q. Xie, M.-R. Chen, J. Weng, Adaptive population extremal optimization-based PID neural network for multivariable nonlinear control systems, *Swarm and Evolutionary Computation*, vol. 44 (2019) 320–334. doi: 10.1016/j.swevo.2018.04.008
- [9] R. Ortega, D. N. Gerasimov, N. E. Barabanov, V. O. Nikiforov, Adaptive control of linear multivariable systems using dynamic regressor extension and mixing estimators: Removing the high-frequency gain assumptions, *Automatica*, vol. 110 (2019) 108589. doi: 10.1016/j.automatica.2019.108589
- [10] S. H. Nagarsheth, S. N. Sharma, Relative Normalized Gain Array-based interaction indicator for non-square multivariable control systems: properties and application, *IFAC-PapersOnLine*, vol. 53, issue 2 (2020) 4032–4037.
- [11] T. Ma, Recursive filtering adaptive neural fault-tolerant control for uncertain multivariable nonlinear systems, *European Journal of Control*, vol. 59 (2021) 274–289. doi: 10.1016/j.ejcon.2020.10.003
- [12] S. Labiod, T. M. Guerra, Adaptive Fuzzy Control for Multivariable Nonlinear Systems with Indefinite Control Gain Matrix and Unknown Control Direction, *IFAC-PapersOnLine*, vol. 53, issue 20 (2020) 8019–8024. doi: 10.1016/j.ifacol.2020.12.2232
- [13] A. M. Shaheen, R. A. El-Sehiemy, M. M. Alharthi, S. S. M. Ghoneim, A. R. Ginidi, Multi-objective jellyfish search optimizer for efficient power system operation based on multi-dimensional OPF framework, *Energy*, vol. 237 (2021) 121478. doi: 10.1016/j.energy.2021.121478
- [14] Q. Zhang, J. Ding, W. Kong, Y. Liu, Q. Wang, T. Jiang, Epilepsy prediction through optimized multidimensional sample entropy and Bi-LSTM, *Biomedical Signal Processing and Control*, vol. 64 (2021) 102293. doi: 10.1016/j.bspc.2020.102293
- [15] A. Mohammadi, F. Sheikholeslam, S. Mirjalili S., Inclined planes system optimization: Theory, literature review, and state-of-the-art versions for IIR system identification, *Expert Systems with Applications*, vol. 200 (2022) 117127. doi: 10.1016/j.eswa.2022.117127
- [16] Vasiliev S., Badamshin R., Valeev S., Vasiliev V., Gvozdev V., Guzairov M., Zhernakov S., Ilyasov B., Kusimov S., Munasyrov R., Raspopov E., Frid A. and Chernyahovskaya L. (2008) Intelligent systems for control and monitoring of gas turbine engines, Ufa, Ufa State Aviation Technical University, 550 p.

- [17] S. Vladov, N. Nazarenko, N. Tutova, V. Moskalyk, A. Ponomarenko, Multi-dimensional TV3-117 aircraft engine automatic control system based of the neural network regulator, Transactions of Kremenchuk Mykhailo Ostrohradskyi National University, issue 2/2020 (121) (2020) 79–84. doi: 10.30929/1995-0519.2020.2.79-84
- [18] T. Shmelova, Yu. Shmelov, S. Vladov, Concept of building intelligent control systems for aircraft, unmanned aerial vehicles and aircraft engines, 2020 IEEE 6th International Conference on Methods and Systems of Navigation and Motion Control (MSNMC), Kiev, Ukraine, October 2020 14–19. doi: 10.1109/MSNMC50359.2020.9255509
- [19] S. Vladov, A. Matusiev, I. Yakovenko, Synthesis of channels for control of helicopters aircraft engines gas generator r.p.m, Physical processes and fields of technical and biological objects: XX International scientific and technical conference, Kremenchuk, Ukraine, November, 2021, 11–13.
- [20] B. Ilyasov, V. Vasilyev, S. Valeev, Design of multi-level intelligent control systems for complex technical objects on the basis of theoretical-information approach, Acta Polytechnica Hungarica, vol. 17, no 8 (2020) 137–150. doi: 10.12700/APH.17.8.2020.8.10
- [21] Y. Shen, K. Khorasani, Hybrid multi-mode machine learning-based fault diagnosis strategies with application to aircraft gas turbine engines, Neural Networks, vol. 130 (2020) 126–142. doi: 10.1016/j.neunet.2020.07.001
- [22] E. Denisova, M. Chernikova, Automatic control system for gas turbine engines with the insertion of mathematical models to the control, Fundamental research, no. 9-2 (2016) 243–248.
- [23] V. Petunin, Synthesis of automatic control systems for gas turbine engines with channel selector, Bulletin of USATU, vol. 11, no 1 (28) (2008) 3–10.
- [24] V. Petunin, A. Frid, Method for constructing adaptive logical-dynamic automatic control systems with selectors, Journal of Instrument Engineering, vol. 54, no 5 (2011) 49–56.
- [25] V. Petunin, Mathematical models of multiconnected automatic control systems with channel selectors, Bulletin of USATU, vol. 15, no 2 (42) (2011) 52–58.
- [26] V. Petunin, Synthesis of automatic control systems for aircraft with automata limiting parameters, Journal of Instrument Engineering, vol. 53, no 10 (2010) 18–24.
- [27] V. Petunin, Synthesis of an adaptive gas-turbine engine gas temperature controller, Reshetnev Readings: Proceedings of the XIII International Scientific Conference, Krasnoyarsk, Russia, November, 2009 158–159.
- [28] I. Elizarov, M. Soludanov, Self-adjustable neural network control system of multilinked dynamic object, Information processes and management, no 1 (2006) 30–44.
- [29] I. Siddikov, Z. Iskandarov, Algorithm for the synthesis of a self-tuning neural network control system for multicomponent dynamic objects, 11th World Conference “Intelligent System for Industrial Automation” (WCIS-2020), Tashkent, Uzbekistan, October, 2021 435–441. doi: 10.1007/978-3-030-68004-6\_57
- [30] Y. Xue, Y. Wang, J. Liang, A self-adaptive gradient descent search algorithm for fully-connected neural networks, Neurocomputing, vol. 478 (2022) 70–80. doi: 10.1016/j.neucom.2022.01.001
- [31] L. Demidova, D. Marchev, Application of recurrent networks in the classification problem of failures in the complex technical systems within the framework of proactive maintenance, Vestnik of Ryazan State Radio Engineering University, no 69 (2019) 135–148. doi: 10.21667/1995-4565-2019-69-135-148
- [32] B. Ilyasov, G. Saitova, I. Sabitov, Control of multi-connected systems based on logic controllers, Bulletin of USATU, vol. 18, no 2 (63) (2014) 98–102.